

See discussions, stats, and author profiles for this publication at: <https://www.researchgate.net/publication/231177327>

Why Superhydrophobic Surfaces Are Not Always Icephobic

ARTICLE *in* ACS NANO · SEPTEMBER 2012

Impact Factor: 12.88 · DOI: 10.1021/nn302138r · Source: PubMed

CITATIONS

49

READS

207

2 AUTHORS:



Michael Nosonovsky

University of Wisconsin - Milwaukee

98 PUBLICATIONS 2,952 CITATIONS

SEE PROFILE



Vahid Hejazi

Rice University

13 PUBLICATIONS 174 CITATIONS

SEE PROFILE

Why Superhydrophobic Surfaces Are Not Always Icephobic

Michael Nosonovsky* and Vahid Hejazi

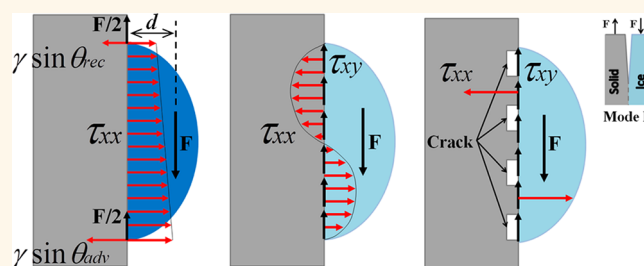
College of Engineering & Applied Science, University of Wisconsin—Milwaukee, Milwaukee, Wisconsin 53211, United States

In several recent papers published in *ACS Nano*,¹ *ACS Applied Materials and Interfaces*,² *Langmuir*,^{3–8} and other journals,^{9–14} it was suggested that surface-roughness-induced superhydrophobicity can be used to design icephobic or anti-icing coatings. The assumption behind this suggestion was that mechanisms of ice and water adhesion are similar, and therefore, by designing a surface with low surface energy (large water contact angle), one can achieve also weak adhesion between the surface and ice. However, the mechanisms of water and ice adhesion are different. Water can withstand pressure, either positive (compressive) or negative (tensile),^{14,15} but it cannot support shear stress since the stress tensor τ of liquid is spherical in the static limit ($\tau_{xy} = 0$).

To understand why superhydrophobic surfaces are not necessarily icephobic, one should investigate mechanical forces acting on a liquid droplet and on ice. There are certain forces applied at the triple line of a droplet placed on a solid surface with the contact radius $r = R \sin \theta$, where R is the curvature radius of the droplet and θ is the contact angle (CA). First, the x -components (tangential components) of interfacial tension forces γ_{SW} , γ_{SA} , and γ_{WA} (where indices S, W, and A stand for solid, water, and air) are balanced as prescribed by the Young equation $\gamma_{WA} \cos \theta + \gamma_{SW} = \gamma_{SA}$ (Figure 1a). The y -component (normal component) is balanced by the Laplace pressure $p_L = 2\gamma_{WA}/R = 2\gamma_{WA} \sin \theta/r$ inside the droplet, so that the solid substrate experiences a concentrated normal force $\gamma_{WA} \sin \theta$ (per unit length) at the triple line and distributed pressure $p = 2\gamma_{WA} \sin \theta/r$ at the contact area πr^2 , which balance each other and can deform the substrate (Figure 1b). For a two-dimensional (2D) droplet, the Laplace pressure is $p_L = \gamma_{WA}/R = \gamma_{WA} \sin \theta/r$, whereas the contact zone is $2r$, so the distributed force of $2\gamma_{WA} \sin \theta$ is balanced by two forces of $\gamma_{WA} \sin \theta$ at the edges of the droplet.

If a shear or normal force F is applied to the droplet (e.g., droplet's weight

ABSTRACT



We discuss mechanical forces that act upon a water droplet and a piece of ice on a rough solid surface and the difference between dewetting and ice fracture. The force needed to detach a water droplet depends on contact angle (CA) hysteresis and can be reduced significantly in the case of a superhydrophobic surface. The force needed to detach a piece of ice depends on the receding CA and the initial size of interfacial cracks. Therefore, even surfaces with very high receding CA may have strong adhesion to ice if the size of the cracks is small.

$F = \rho g(\pi/3)R^3(1 - \cos \theta)^2(2 + \cos \theta)$ for a truncated sphere), then the droplet is deformed, and CA hysteresis $\Delta\theta = \theta_{adv} - \theta_{rec}$ occurs so that the applied force is balanced by the difference of the CAs at the advancing and receding edges due to CA hysteresis. The balance of the x -components of the forces applied to the droplet is given by the tangential component of the force ($\gamma_{WA} \cos \theta_{adv}$ at the advancing edge and $\gamma_{WA} \cos \theta_{rec}$ at the receding edge) multiplied by the width of the droplet $2r$ ¹⁶

$$F_x = 2r\gamma_{WA}(\cos \theta_{rec} - \cos \theta_{adv}) \quad (1)$$

Similarly, one can argue that the y -component is given by

$$F_y = 2r\gamma_{WA}(\sin \theta_{adv} + \sin \theta_{rec}) - \pi r^2 p_L \quad (2)$$

The shear force also creates the gradient in the hydrostatic pressure along the interface, $p(x) = p_L + \rho g x$ from the top to the bottom of the droplet. Since the droplet is in equilibrium, the total moment of forces acting upon the droplet is equal to zero. For a 2D droplet, the moment (per unit length) is

* Address correspondence to nosonovs@uwm.edu.

Published online September 25, 2012
10.1021/nn302138r

© 2012 American Chemical Society

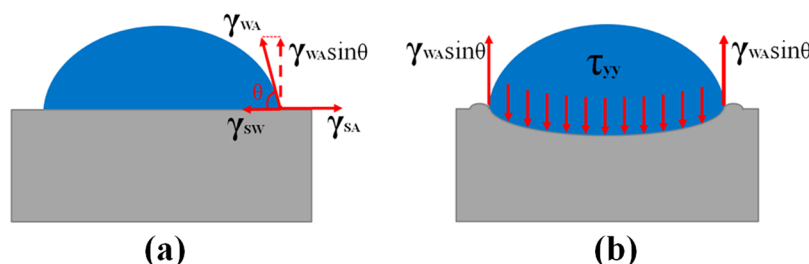


Figure 1. Surface tension forces at the edge of a water droplet: (a) the tangential components of γ_{WA} is balanced by the interfacial tensions, whereas (b) the normal component is balanced by the Laplace pressure.

calculated as

$$M = \gamma_{WA}r(\sin\theta_{adv} - \sin\theta_{rec}) + \int_{-r}^r \rho g x dx - f_x d = 0 \quad (3)$$

where d is the offset at which the force f_x per unit length (analogous to F_x for a three-dimensional (3D) droplet) is applied; for example, d is the position of the center of masses of the droplet. For a 3D droplet, the calculation is more complex; however, it involves the same principle.

Mathematically, the three equations of equilibrium prescribe the values of F_x , F_y , and $F_x d$ for a given value of $\Delta\theta$; however, physically, the applied loads define the deformation of the droplet and, therefore, $\Delta\theta$. From the mechanical point of view, a system with the number of constraining equations greater than the number of unknowns is a statically indeterminate system. To solve the paradox of the overconstrained system, we should realize that, when the external load is applied, the droplet deforms, and therefore, the value of offset can change and the mean curvature changes affecting the Laplace pressure p_L . As a result, the system of three equilibrium equations of equilibrium determines three unknowns: $\Delta\theta$, p_L , and d .

The dewetting occurs when the applied force results in $\Delta\theta$, which exceeds this maximum value. Equations 1–3 can be simplified with the use of trigonometric identities as

$$\begin{aligned} F &= 2r\gamma_{WA}(\cos\theta_{adv} - \cos\theta_{rec}) \\ &= 4r\gamma_{WA}\sin\theta_0\sin\frac{\theta_{adv} - \theta_{rec}}{2} \\ &\approx 2R\gamma_{WA}(\sin\theta_0)^2\Delta\theta \end{aligned} \quad (4)$$

where $\theta_0 = (\theta_{adv} + \theta_{rec})/2$ (for small hysteresis, $\theta_0 = \theta$). For a typical droplet with the contact radius of $R = 1$ mm, $\sin^2\theta_0 = 0.5$, $\gamma_{WA} = 0.07$ N/m, and CA hysteresis $\Delta\theta = 0.1$ rad, the shear force needed to move the droplet is estimated as $F = 7$ μ N. It is also observed that the effect of superhydrophobicity is two-fold: the reduction of $\sin\theta_0$ and the reduction of $\Delta\theta$ because the superhydrophobicity implies both high CA and small CA hysteresis.

The situation changes when the droplet freezes. Ice can support shear load τ_{xy} and a distributed normal stress τ_{yy} , which balances the torque created by the shear force F_x applied at the offset d . However, ice detachment from a solid surface occurs through fracture, and therefore, it is different from the dewetting mechanism. Fracture can occur within the ice itself when the interface with the substrate is strong or at the substrate–ice interface if defects (e.g., cracks) are present.¹⁷ Fracture occurs in accordance with the mode I (opening) or mode II (edge sliding) cracking scenarios, which correspond to normal and shear loading.¹⁸ The critical strength above which the fracture occurs in mode I is given by

$$\tau_{yy} = \sqrt{\frac{EG}{\pi a}} \quad (5)$$

where E is the Young modulus, G is the surface energy of the crack, and a is the crack length. The analysis for mode II crack fracture is similar. Typically, it is assumed that the surface energy has a constant value $G = \gamma_{SA} + \gamma_{IA} - \gamma_{SI}$, where γ_{IA} and γ_{SI} are the ice–air and solid–ice interfacial

energies. However, a more detailed analysis shows that the value of surface energy depends on whether it is measured during the approach of two surfaces or during their separation. This is because of the so-called adhesion hysteresis.¹⁹ The energy needed to separate surfaces is greater than that gained by bringing them together. Adhesion hysteresis is related to CA hysteresis, so that the former is one of the underlying causes of the latter.²⁰

Note the analogy with the Young equation

$$G = \gamma_{IA}(1 + \cos\theta) \quad (6)$$

where $\cos\theta = (\gamma_{SA} - \gamma_{SI})/\gamma_{IA}$. If the interfacial energies of two phases of water are close to each other, $\gamma_{IA} \approx \gamma_{WA}$ and $\gamma_{SI} \approx \gamma_{WI}$, then the values of θ for water and ice are also comparable and thus superhydrophobicity corresponds to a high value of θ for ice. During the detachment of the solid surfaces or opening the crack, the energy of separation matters, which is related to the receding CA, as opposed to the energy of bringing the surfaces together, which is related to the advancing CA. Therefore, when the crack is opening, only the receding value matters, $G_{rec} = \gamma_{IA}(1 + \cos\theta_{rec})$. The critical stress is related to the receding CA as

$$\begin{aligned} \tau_{yy} &= \sqrt{\frac{EG_{rec}}{\pi a}} \\ &= \sqrt{\frac{E\gamma_{IA}(1 + \cos\theta_{rec})}{\pi a}} \end{aligned} \quad (7)$$

From eq 7, we conclude that (i) shear strength correlates with the receding contact angle; (ii) superhydrophobic surface has low shear

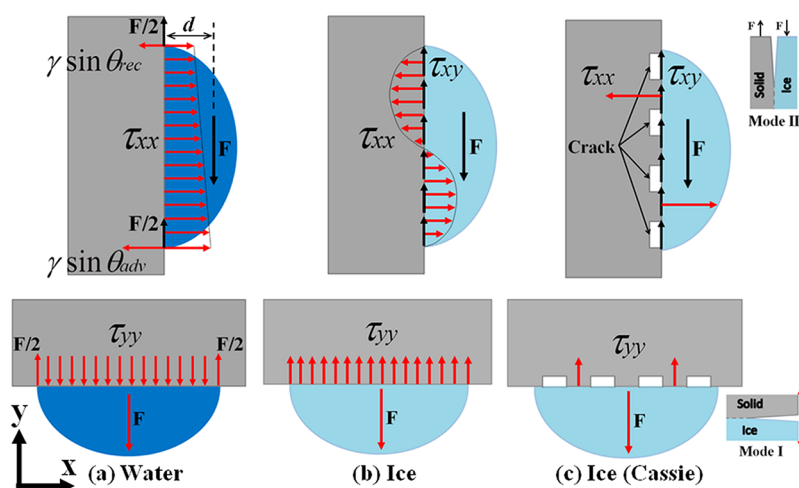


Figure 2. Normal (red) and shear (black) forces during shear loading of (a) water droplet and (b) ice frozen droplet on a flat and (c) textured (Cassie state) surface in the regime of the tangential and normal loading.

strength because high CA, $\theta_{\text{rec}} \rightarrow 180^\circ$, corresponds to low values of $1 + \cos \theta_{\text{rec}}$; and (iii) the effect of initial crack size is very significant. Thus, for the values of $E = 9.7$ GPa, $\gamma_{\text{IA}} = 0.109$ N/m,²¹ $\cos \theta_{\text{rec}} = -0.9$, and $a = 100$ μm , the shear strength is $\tau_{yy} = 58$ kPa. For an ice particle with the contact area of 1 mm^2 , this corresponds to the shear force of 58 mN, which is about 4 orders of magnitude larger than for a droplet. For a superhydrophobic surface with the same properties but smaller cracks of $a = 1$ μm , the force will be 580 mN. For hydrophilic surfaces, roughening the surface can increase its adhesion to ice, as water penetrated the cavities between the asperities. However, most superhydrophobic surfaces are in the so-called Cassie state, with air pockets trapped between the solid and water droplet. When water freezes, the pockets become air voids and they can serve as stress concentrators. While superhydrophobic surfaces can be beneficial to prevent ice formation through condensation of water droplets, ice shedding should be targeted for robust icephobicity. It is therefore desirable to have a surface that supports both the Cassie superhydrophobic regime and crack formation in ice. In addition, many superhydrophobic surfaces have dual tier roughness; however, the effect of dual tier on ice adhesion shedding should be investigated separately.

We conclude that the superhydrophobic state by itself can affect the crack opening energy; however, the Cassie wetting state can decrease the shear strength by introducing voids between the solid surface and water/ice, which serve as microcracks (stress concentrators) and increase a . Although icephobic properties correlate with high receding CA, the size of the microcracks at the solid–ice interface is the critical parameter that governs ice adhesion to a hydrophobic solid. Consequently, some superhydrophobic surfaces can have strong ice adhesion if they do not provide sufficiently large voids at the interface.

REFERENCES AND NOTES

- Meuler, A. J.; McKinley, G. H.; Cohen, R. E. Exploiting Topographical Texture To Impart Icephobicity. *ACS Nano* **2010**, *4*, 7048–7052.
- Meuler, A. J.; Smith, J. D.; Varanasi, K. K.; Mabry, J. M.; McKinley, G. H.; Cohen, R. E. Relationships between Water Wettability and Ice Adhesion. *ACS Appl. Mater. Interfaces* **2010**, *11*, 3100–3110.
- Zheng, L.; Li, Z.; Bourdo, S.; Khedir, R. K.; Asar, M. P.; Ryerson, C. C.; Biris, A. S. Exceptional Superhydrophobicity and Low Velocity Impact Ice phobicity of Acetone-Functionalized Carbon Nanotube Films. *Langmuir* **2011**, *27*, 9936–9943.
- Jung, S.; Dorrestijn, M.; Raps, D.; Das, A.; Megaridis, C. M.; Poulidakos, D. Are Superhydrophobic Surfaces Best for Icephobicity? *Langmuir* **2011**, *27*, 3059–3066.
- Kulinich, S. A.; Farhadi, S.; Nose, K.; Du, X. W. Superhydrophobic Surfaces: Are They Really Ice-Repellent? *Langmuir* **2011**, *27*, 25–29.
- Bahadur, V.; Mishchenko, L.; Hatton, B.; Taylor, J. A.; Aizenberg, J.; Krupenkin, T. Predictive Model for Ice Formation on Superhydrophobic Surfaces. *Langmuir* **2011**, *27*, 14143–14150.
- Cao, L.-L.; Jones, A. K.; Sikka, V. K.; Wu, J.; Gao, D. Anti-Icing Superhydrophobic Coatings. *Langmuir* **2009**, *25*, 12444–12448.
- Kulinich, S. A.; Farzaneh, M. How Wetting Hysteresis Influences Ice Adhesion Strength on Superhydrophobic Surfaces. *Langmuir* **2009**, *25*, 8854–8856.
- Dotan, A.; Dodiuk, H.; Laforte, C.; Kenig, S. The Relationship between Water Wetting and Ice Adhesion. *J. Adhes. Sci. Technol.* **2009**, *23*, 1907–1915.
- Menini, R.; Ghalmi, Z.; Farzaneh, M. Highly Resistant Icephobic Coatings on Aluminum Alloys. *Cold Reg. Sci. Technol.* **2011**, *65*, 65–69.
- Farhadi, S.; Farzaneh, M.; Kulinich, S. A. Anti-Icing Performance of Superhydrophobic Surfaces. *Appl. Surf. Sci.* **2011**, *257*, 6264–6269.
- Wong, T.-S.; Kang, S. H.; Tang, S. K. Y.; Smythe, E. J.; Hatton, B. D.; Grinthal, A.; Aizenburg, J. Bioinspired Self-Repairing Slippery Surfaces with Pressure-Stable Omniphobicity. *Nature* **2011**, *477*, 443–447.
- Yang, S. H.; Nosonovsky, M.; Zhang, H.; Chung, K.-H. Nanoscale Water Capillary Bridges under Deeply Negative Pressure. *Chem. Phys. Lett.* **2008**, *451*, 88–92.
- Nosonovsky, M.; Bhushan, B. Phase Behavior of Capillary Bridges: Towards Nanoscale Water Phase Diagram. *Phys. Chem. Chem. Phys.* **2008**, *10*, 2137–2144.
- Nosonovsky, M. Slippery When Wetted. *Nature* **2011**, *477*, 412–413.
- de Gennes, P. G.; Brochard-Wyart, F.; Quere, D. *Capillary and Wetting Phenomena: Drops, Bubbles, Pearls, Waves*; Springer-Verlag: New York, 2004.

17. Raraty, L. E.; Tabor, D. The Adhesion and Strength Properties of Ice. *Proc. R. Soc. A* **1958**, *245*, 184–201.
18. Anderson, T. L. *Fracture Mechanics: Fundamentals and Applications*; CRC Press: Boca Raton, FL, 1995.
19. Israelachvili, J. N. *Intermolecular and Surface Forces*, 2nd ed.; Academic Press: London, 1992.
20. Nosonovsky, M.; Bhushan, B. *Multi-scale Dissipative Mechanisms and Hierarchical Surfaces: Friction, Superhydrophobicity and Biomimetics*; Springer-Verlag: Heidelberg, 2008.
21. Petrovic, J. J. Review: Mechanical Properties of Ice and Snow. *J. Mater. Sci.* **2003**, *38*, 1–6.